A Primer on MRI and Functional MRI

(version 2.1, 6/21/01)

Douglas C. Noll, Ph.D.
Departments of Biomedical Engineering and Radiology
University of Michigan, Ann Arbor, MI 48109-2125
dnoll@umich.edu

Abstract

Functional brain mapping with magnetic resonance imaging (MRI) is a rapidly growing field that has emerged in only the past several years. Functional MRI (fMRI) is the use of MRI equipment to detect regional changes cerebral metabolism or in blood flow, volume or oxygenation in response to task activation. The most popular technique utilizes blood oxygenation level dependent (BOLD) contrast, which is based on the differing magnetic properties of oxygenated (diamagnetic) and deoxygenated (paramagnetic) blood. These magnetic susceptibility differences lead to small, but detectable changes in susceptibility-weighted MR image intensity. Relatively low image signal-to-noise ratio (SNR) of the BOLD effect, head movement, and undesired physiological sources of variability (cardiac, pulmonary) make detection of the activation-related signal changes difficult. Fortunately, rapid image acquisition techniques can be used to generate data sets with hundreds of images for each slice location which can be statistically analyzed to determine foci of brain activity. Finally, the basic properties of the human activation response have implications for experimental design and statistical processing techniques used for extraction of functional information from the four-dimensional data sets.

An Introduction to NMR

Magnetic resonance imaging (MRI) has been used for over 15 years to generate exquisite images of the soft tissue anatomy of the human body. Only recently has MRI been employed to image the functioning human brain in a completely non-invasive fashion contrast [1-4]. MRI is based on the physics of Nuclear Magnetic Resonance or NMR, a property of atomic nuclei that was discovered in the 1940's and has a long history of use in chemical analyses. The NMR phenomenon is based on the quantum mechanical property of nuclear spin. Nuclei having an odd number of neutrons, odd number of protons, or both will have a net magnetic moment and will therefore be NMR active. Among the most commonly used nuclei are ^{1}H, ^{13}C, ^{19}F, ^{23}Na, and ^{31}P. For imaging in biological systems, ^{1}H or "proton" NMR is the most common, primarily due to its high concentration in the human body and high sensitivity (it gives rise to very large NMR signals).

Consider an object that contains many hydrogen nuclei, each with the characteristic nuclear spin. In an NMR experiment, the object to be imaged is placed in a large, static magnetic field. The magnetic field is commonly supplied by a superconducting magnet that remains "on" continuously, often for several years at a time. The magnetic moments associated with nuclear spin tend to align themselves parallel or anti-parallel to the static magnetic field, $\mathbf{B_0}$ (this is

equivalent to spins residing in low or high energy states, respectively). A slightly larger fraction aligns parallel to the main magnetic field forming a net magnetization (**M**) parallel to the magnetic field as shown in Figure 1.
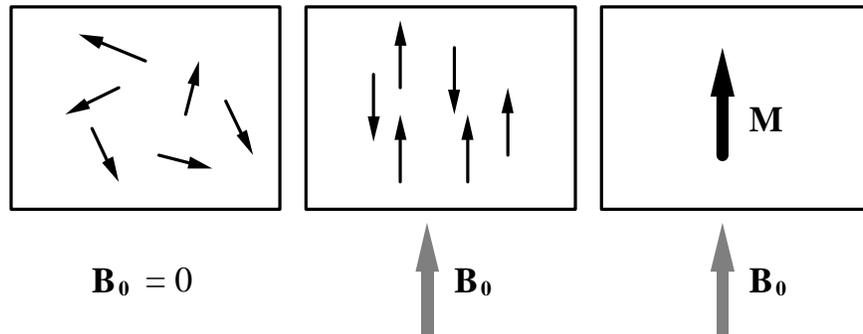

$$\mathbf{B_0} = 0 \qquad \mathbf{B_0} \qquad \mathbf{B_0}$$

Figure 1. Randomly oriented magnetic moments aligning with an applied magnetic field (**B$_0$**) to form a net magnetization.

The magnetization demonstrates a resonance phenomenon to oscillating magnetic fields at a characteristic frequency determined by the Larmor relationship:

$$f = \gamma\,\mathbf{B}_0 \qquad (1)$$

where B_0 is the strength of the applied magnetic field, and γ is a proportionality constant specific to the nuclear species. For example, with ^{1}H or protons, $\gamma = 42.58$ MHz/T and if the magnetic field is 1.5 T, then the resonant frequency is 63.76 MHz. Because of this resonance phenomenon, if an oscillating magnetic field at this resonance frequency is applied to the object, then the spins will absorb energy and become excited. The oscillating magnetic field is called an radio frequency (RF) field because the frequencies are similar to those used in radio transmission. This process, know as excitation, results in the magnetization being partially or completely tipped the into the plane perpendicular to main magnetic field. Once excited, the magnetization precesses around the static magnetic field at its resonant frequency given in Equation (1), above. A coil placed near to the object can detect this precessing magnetization as shown in Figure 2.
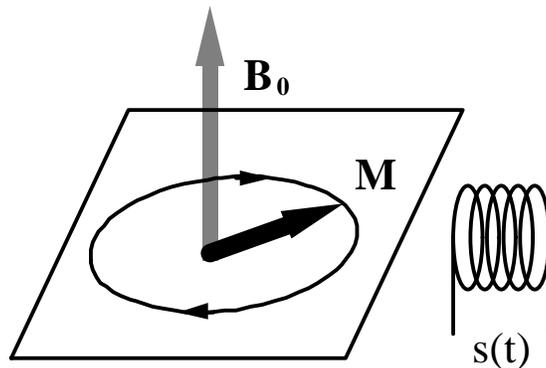

Figure 2. Excited magnetization precessing around the static magnetic field thus inducing a voltage, s(t), in a nearby coil.

Following excitation, the magnetization returns to its equilibrium state according to exponential decay processes. The magnetization precessing in the plane perpendicular to the static field, decays exponentially with the time constant, T_2. The mechanism underlying this decay term is incoherent (and unrecoverable) phase dispersal of the signal due interactions between nuclear spins. In the presence of an inhomogeneous magnetic field, spins will have differing precessing rates induced by this inhomogeneity also causing phase dispersal and more rapid signal decay. The decay of magnetization including both T_2 (spin-spin interactions) and magnetic field inhomogeneity is given a time constant called T_2^*. Finally, the magnetization returns to its equilibrium state, aligned to the main magnetic field with time constant, T_1. Much of MRI is based on exploiting differences in these parameters to develop image contrast between different tissues.

A good analogy for the resonance phenomenon is a guitar string. Here the frequency varies according to the tension on the string (rather than the strength of the magnetic field). This string is commonly plucked to excite it, but it can also be excited by holding a loudspeaker near to the string and playing a note at the same frequency as the string. The latter case is similar in manner to the way in which nuclear spins are excited. The acoustic waves coming off of the string will then slowly decay away. This is just like the T_2 decay.

Localization in One Dimension

Spatial localization in MRI is accomplished by a controlled manipulation of the magnetic field [5]. Based on the Larmor relationship of Equation (1), a spatially variant magnetic field will lead to a spatially variant distribution of resonant frequencies. Since precessing magnetization from the entire object induces signal changes in the receiver coil, the received signal now contains a spectrum of received signals. Frequency analysis can then be used to discriminate between different spatial locations based on the spatial distribution of magnetic field strength. Typically, specially designed electrical coils are used to induce a magnetic field manipulation that varies linearly with spatial location:

$$B(x) = B_0 + G{\cdot}x \qquad (2)$$

where G is the slope or "gradient" of the strength of the magnetic field. This additional magnetic field described by G is called a gradient magnetic field. Since this gradient is applied in the x direction, this is called an x-gradient (G_x). Using Equation (1), the frequency distribution is now:

$$f(x) = \gamma\,(B_0 + G{\cdot}x). \qquad (3)$$

There is now a one-to-one correspondence of spatial location in the x direction with frequency of precession as shown in Figure 3(a). If we take the received signal (e.g. s(t) from Fig. 2) and generate its spectrum, then we get a picture of what the distribution of the magnetization as a function of spatial location, as shown in Figure 3(b). Relating frequency to spatial location is very common in MRI and is given the term "frequency encoding."

The mathematical relationship that converts a signal (e.g. s(t)) into its spectrum is called the Fourier transform. The one-dimensional (1D) Fourier transform of the signal, therefore, gives the one-dimensional distribution of magnetization in the x direction (if you will, a 1D image). The intensity of the image (e.g. the height of the curve in Fig. 3(b-lower)) defines how much magnetization exists at that particular x position.
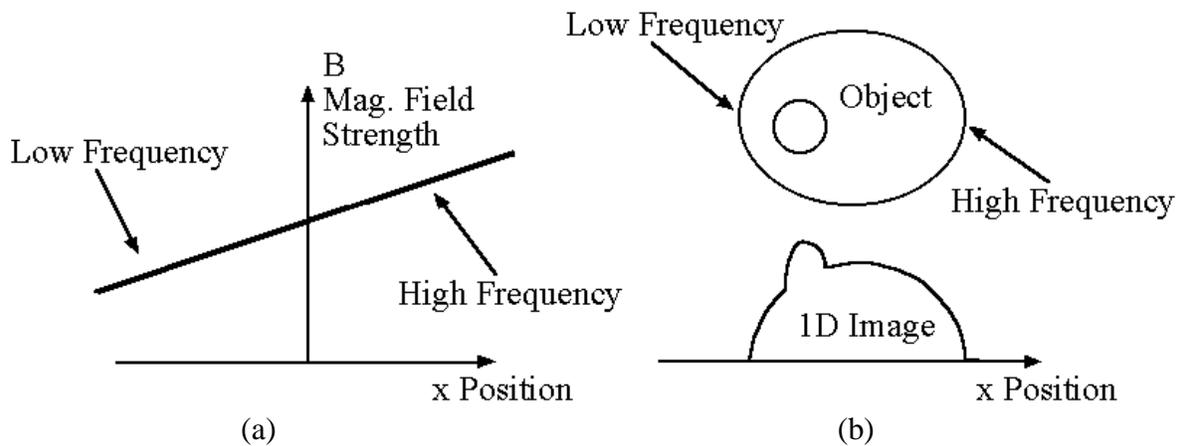
3

Figure 3. (a) Frequency distribution as a function of position. (b-upper) Frequencies in an object and (b-lower) the corresponding spectrum.

Pulse Sequences

Every NMR imaging experiment is governed by a computer program called a "pulse sequence," which is simply a list of instruction the various experimental units. Figure 4 contains a pulse sequence diagram of a 1D imaging experiment. The elements are as follows: first an RF pulse is applied to excite the magnetization and then the x-gradient is applied to set up the correspondence between frequency and spatial location (in x) (frequency encoding). During the frequency encoding, the received signal (e.g. s(t)) is sampled by the data acquisition unit. As described above, a 1D image is created by taking the Fourier transform of this sampled data. Finally, after the signal has decayed away (T_2) and the magnetization has recovered (T_1), the process is repeated (to allow some different encoding, averaging, a different slice, etc.).
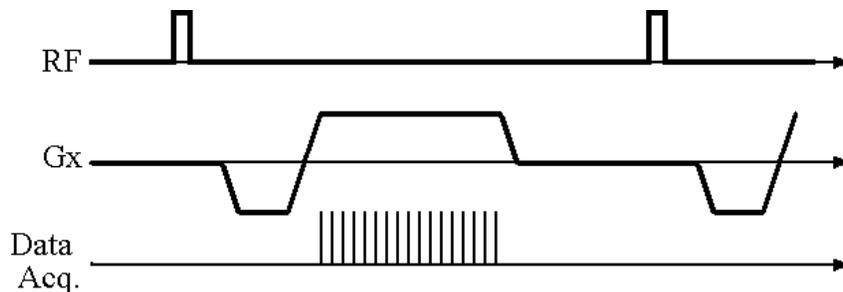

Figure 4. 1D Localization pulse sequence.

Once nice analogy for a precessing nucleus is the rotation of the hand of a clock. Fast precession means faster rotation of the clock hand. In Figure 3, for example, a clock on the right side would rotate faster than a clock on the left side. An interesting feature is that precession (or rotation) of the nuclei is completely determined by the applied magnetic field. For example, turning the gradient off can almost instantly stop the situation where the right side of the object is at a higher frequency than the left side (Figure 3). It can also be restarted just as quickly. The precession can be started and stopped as the gradients are commanded to start and stop. Figure 5 contains another pulse sequence that will have almost exactly the same data as in Figure 1.
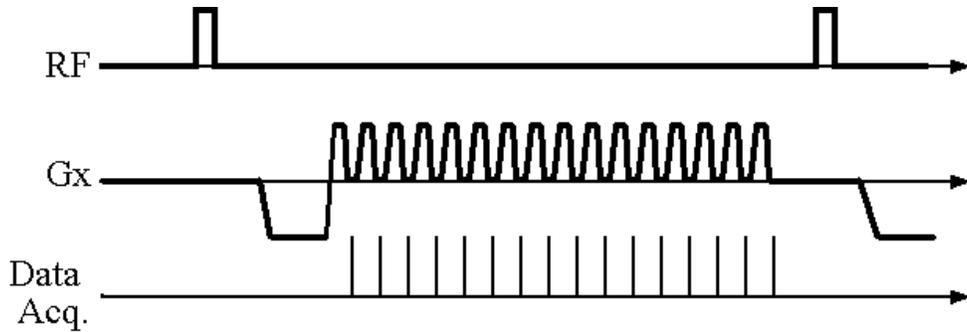
4

Figure 5. Alternate method for 1D localization (one method for phase encoding).

In Figure 4, the nuclei are precessing in a very smooth and uniform fashion while in Figure 5, the nuclei are precessing in more of a "stop-action" or jerky motion. Nevertheless, because the gradient was turned on for the same amount of time between data acquisition samples, the sampled data will be the same. In this method, there is no gradient turned on during each data acquisition so all positions in space have the same precession frequency. Therefore, we can't call this frequency encoding. Instead, we observe that past history of gradients is frozen into the phase of the nuclei. We therefore refer to this method as "phase encoding." As before, if we take the Fourier transform of the sampled data, we'll get a 1D image of the object.

Localization in Two Dimensions (Imaging)

Localization in 2D cannot be performed by simply turning on two gradients (for example, the x and y gradients) at the same time (this will lead to a gradient in a direction halfway between x and y – at 45°). Instead, the two gradients must be applied in a precise sequence. One thing that can be done is to merge the two 1D imaging schemes described above (Figures 4 and 5). For example, we can use the frequency encoding method of Figure 4 in the x direction and the phase encoding method of Figure 5 in the y direction. Here we will place a frequency encoding between each phase encoding step. The pulse sequence for this method is shown in Figure 6. There are many different ways to encode the object data in two dimensions – this method, called Echo Planar Imaging (EPI) [6, 7], is one that is commonly used in functional MRI.
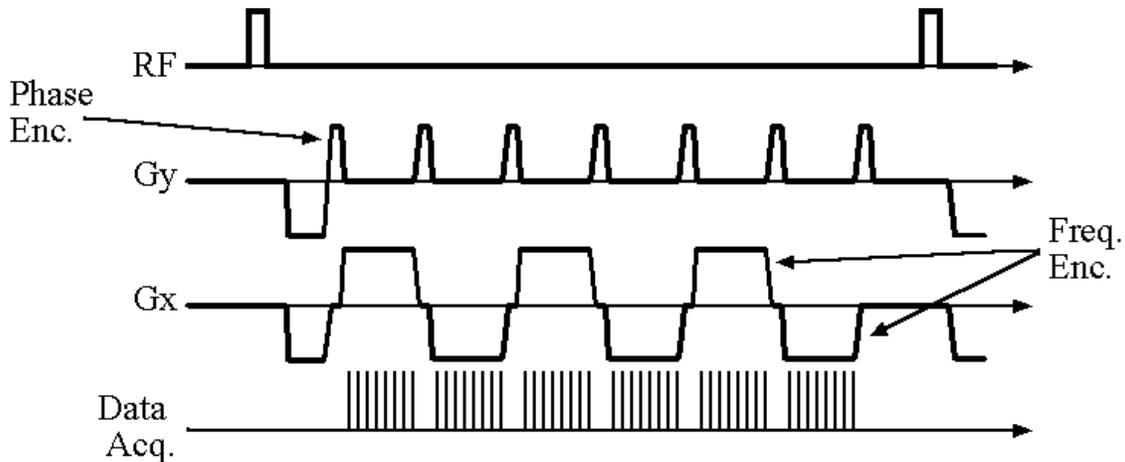

Figure 6. The EPI pulse sequence with phase encoding gradient (Gy) and frequency encoding gradient (Gx).

5

Commonly we structure the acquired data in a two dimensional grid that is called "k-space." This is shown below in Figure 7. There is some elegant mathematics to describe how data are placed into k-space [8-10], but in general, the data acquired form a continuous pathway through the k-space data, which is sometimes called a k-space trajectory. The EPI pulse sequence is uniquely characterized by a "zig-zag"-like pathway that goes back and forth rapidly in the frequency direction (k_x) and moves slowly in the phase direction (k_y). We previously discussed that the Fourier transform can be used to convert the acquired data into its spectral equivalent for both frequency encoding and phase encoding data. As shown above in Figure 3, the spectrum represents spatial position. Here we apply the Fourier transform in both frequency and phase directions obtain the 2D spatial map of MRI data, which is simply an MR image.
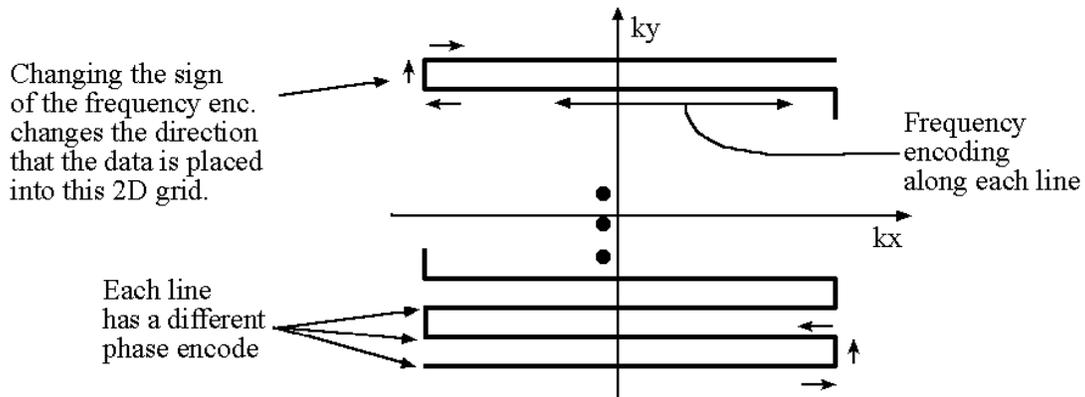

Figure 7. k-space data for the EPI pulse sequence with phase encoding direction (ky) and frequency encoding direction (kx). Taking the Fourier transform in both directions produces the MR image.

Creating an MRI image requires sampling the 2D k-space with sufficient density over a specified extent. The Nyquist sampling theorem dictates the level of sampling density necessary to prevent spatial aliasing of the reconstructed object (parts of the object can alias to different locations). The extent of the acquisition in Fourier space dictates the high-spatial frequency content and hence, the spatial resolution. One feature that distinguishes different image acquisition methods is how quickly one can acquire data for an image and how easily the methods can be extended to generate higher spatial resolution. The EPI method is well known as a very fast method that generally has poor spatial resolution.

The last part of the puzzle is how slices are excited. We describe above how to generate a 2D image, but most humans are 3D. The most common way of dealing with the third dimension is with slice-selective excitation. Remember, if we apply an oscillating (RF) magnetic field at the resonant frequency of a nucleus, then it will become excited. If the RF field is not at the resonant frequency, then no excitation occurs. If we apply a gradient in the z direction, then we can make the resonant frequency vary as a function of z position. Now, when the RF field is applied, it will match the resonant frequency only for a plane at a particular z location. Thus only a plane (or slice) will be excited. Other slices can be excited by shifting the RF frequency up or down, or by shifting the overall magnetic field up or down. Finally, any of the three directions (x, y, or z) can be interchanged and in fact, this coordinate system can be arbitrarily rotated in 3D to achieve any obliquely oriented slices that you may desire.

Introduction to Functional MRI

The physiology of neuronal activity involves many complex processes. It has been established, as long ago as 1890 [11], that physiological functions in the brain respond regionally to brain activity. Magnetic resonance has the capability to measure parameters related to several of these physiological functions, including changes in phosphorus metabolism and metabolic byproducts, blood flow, blood volume, and blood oxygenation. The most common technique uses blood oxygen level dependent (BOLD) contrast [1-4]. This technique is based on the magnetic susceptibility of hemoglobin (Hb). Deoxygenated Hb is paramagnetic, while fully oxygenated Hb is diamagnetic. The presence of the paramagnetic deoxy-Hb distorts the static magnetic field. Spins in this non-uniform magnetic field now precess at different frequencies causing more rapid phase dispersal and decay of the NMR signal. Therefore, changes in blood oxygenation can cause changes in the MR decay parameter, T_2^*, leading to changes in image intensity in T_2^*-weighted images. Table 1, below summarizes the changes in physiology and MR parameters that enable MRI to detect signal changes based on blood oxygenation.

Table 1. Focal physiological and MR parameter changes resulting from cortical activation.

Blood Flow	↑↑↑
O_2 Utilization	↑
Blood O_2 Level	↑↑
Deoxy-Hemoglobin Level	↓↓
Distortions to B_0	↓↓
Phase dispersal of **M**	↓↓
Effective Decay Rate ($1/T_2^*$)	↓↓
T_2^*-weighted Signal	↑↑

The relatively straight forward story is, unfortunately, oversimplified. To give some idea of the complexity of the physiological and physical response of this fMRI signal, refer to Figure 8, below (adapted from Springer, et al. [12]). In this figure, the connecting arrows describe the effect of one parameter on another. Positive/negative arrows indicate positive/negative correlations between the parameters. For example, a increase in blood flow with no other effects would lead to an increase in blood oxygenation while an increase in oxygen metabolism would lead to decrease in blood oxygenation. The rightmost pathway through the diagram is the dominant pathway of physiological and physical effects leading the positive change in BOLD signal in fMRI. One might notice that there are some pathways that have a net negative effect on the signal – as described above, the increase in oxygen metabolism leads to decrease in blood oxygenation, which reduces the fMRI signal. Increases in blood volume will increase the amount of deoxyhemoglobin which makes the magnetic field less uniform and also reduced the fMRI signal. The positive signal changes seen in fMRI studies rely on the dominance of the increase in blood flow over changes in blood volume and oxygen utilization. Further adding to the complexity of the MR signal is an interaction between the observed MRI signal and physical properties such as vessel diameter, orientation, hematocrit and blood volume fraction.

T2*-weighted
Image Intensity

(+)

MR Properties

Decay Time (T2*)

(+)

Physical Effects

Magnetic Field
Uniformity (microscopic)

Other Factors
Vessel Diameter
Vessel Orientation
Hematocrit
Blood Volume Fraction

(-)   (+)

Physiological Effects

Cerebral Blood
Volume (CBV)

Blood
Oxygenation

(+)   (+)

(+)   (-)

Cerbral Blood
Flow (CBF)

(+)

Metabolic Rates

Glucose and Oxygen
Metabolism

(+)

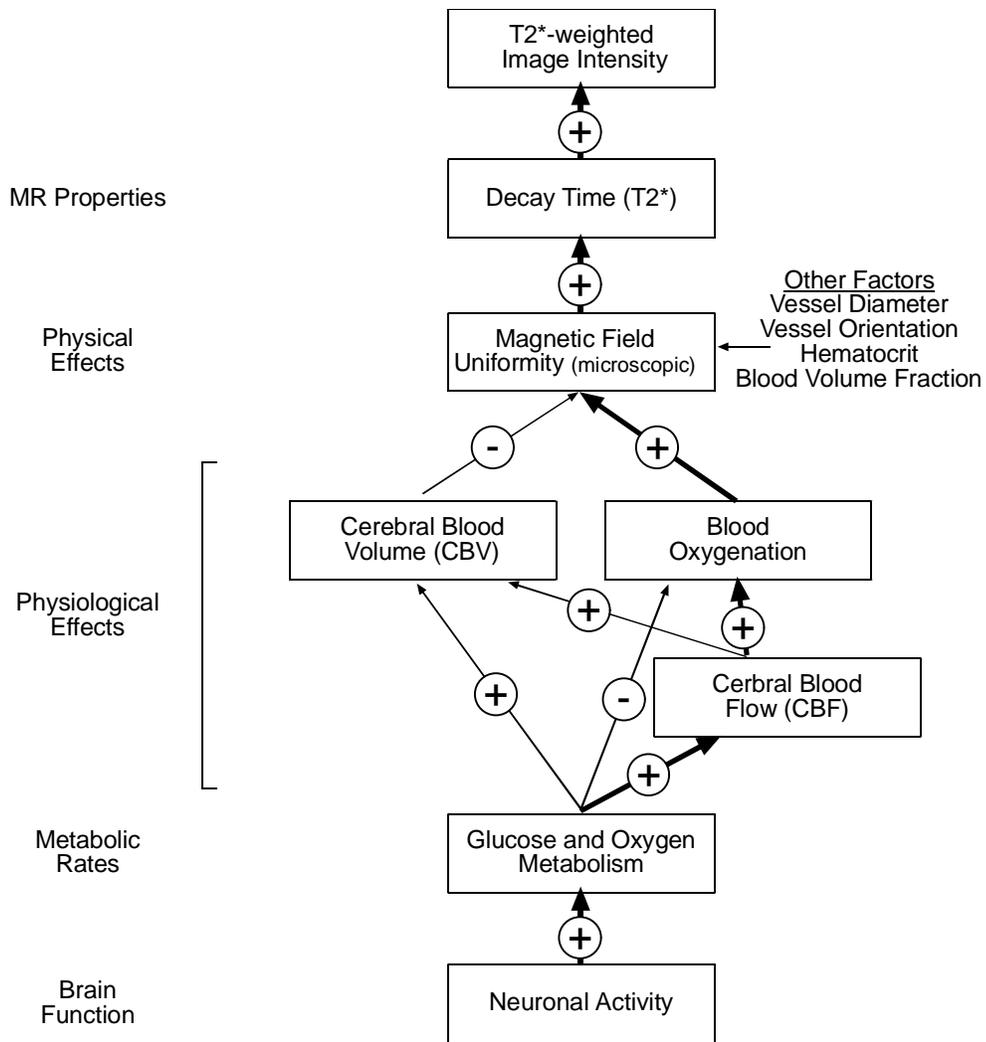**Brain Function**

Neuronal Activity

Figure 8. Schematic of interactions in the formation of the BOLD signal. Positive/negative arrows indicate positive/negative correlations between the parameters. The right most pathway (in bold arrows) is the most significant effect in most BOLD fMRI.

In a typical functional MRI experiment, two or more behavioral conditions are compared and the images are compared to define the regions of the brain that are different between the two conditions.   Since the deoxy-Hb effect is quite small it is typically not visible in a single experimental condition, but can be identified only after subtraction from a different condition. This is sometimes referred to as the subtractive methodology. The images for a hand clenching task and a resting condition can be seen in Figure 9. Only after generating an average subtraction image or a map of a statistical parameter (e.g. a pixel-by-pixel t-test comparison between the conditions), are the regions of activity visible. These regions can be superimposed onto high resolution images or rendered volumes in order to identify the anatomical structures in the brain that are activated.
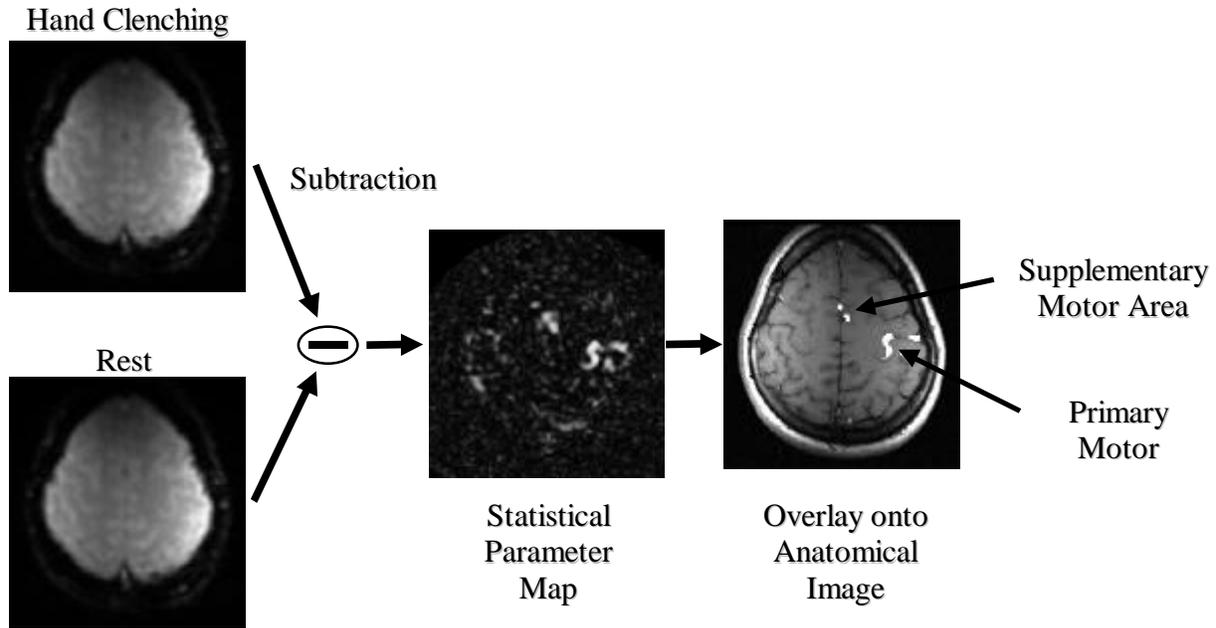
Figure 9. Graphical description of a functional MRI experiment: images from two behavioral conditions are subtracted to yield regions of brain activity. In this case, a hand clenching task was used to define the primary and supplementary motor control areas in the brain.

Noise Issues

Perhaps the most significant technical challenge in functional MRI is the small size of the activation related response. This has commonly been reported to be in the 1-4% range for imaging at the most common magnetic field strength - 1.5 Tesla. Noise in functional MRI comes from a variety of sources. In most MR imaging, the standard sources of noise are thermal noise from the subject (the human body is full of ions and electrons bouncing around generating electromagnetic noise), reception coil, preamplifiers and other electronics, and quantization noise from the analog to digital conversion. In functional MRI, it as also been observed that there are variations in the received signal that correlate strongly with the respiratory and cardiac cycles. These sources have been verified through independent acquisition of respiration and cardiac signals from a blood pulse oximeter and pneumatic systems for monitoring chest wall movement.

Another significant source of signal variations in functional MRI is head movement. Consider an object edge in which image intensity change of ΔI. A fractional pixel movement of size ΔX, can cause the image intensity to vary by about $\Delta I \times \Delta X$. At an object boundary, then, movements that are a small fraction of pixel can cause signal changes that are greater than the activation response of 1-4%. For common pixel dimensions of 1-3 mm, even a movement of 100 μm is problematic. There are also a variety of very slow signal drifts in image intensity that have been observed. These drifts, which appear in human subjects but not in inanimate phantoms, have a time course characterized in several to tens of minutes and are spatially variant. The suspected sources of these signal drifts include physiological state of the subject, equipment instability, and settling of the head into padding. Finally, uncontrolled or spontaneous neuronal events represents yet another source of noise. In the context of a functional imaging study this source of noise includes differences in the manner in which a task is

9

performed, neuronal events associated with behavior (conscious or otherwise) unrelated to the task, and spontaneous firing of networks (consolidation processes, etc.).

There are a number of approaches to addressing noising fMRI data. First, all of the standard methods for improve the signal-to-noise ratio (SNR) with respect to thermal noise also apply to fMRI. This include using special reception coils, for example those designed to receive from specific parts of the brain, and using high field scanners, which increases the equilibrium magnetization as well as increasing the magnetic field non-uniformity's from the paramagnetic effects of deoxy-Hb (increases the size of the fMRI signal changes). In addition to these hardware solutions, one can commonly trade spatial and temporal resolution for improved SNR. In one formulation, the SNR equation for an MR image is:

$$\text{SNR} = \text{M V } \sqrt{T_{A/D}}$$

The parameter M in this relationship is the magnetization, which is a function of tissue parameters (T_1, T_2 or T_2^*, spin density), imaging parameters (T_R, T_E, flip angle), and field strength, B_0. The parameter V is the voxel volume and $T_{A/D}$ represents the total time spent sampling k-space for a given image. Clearly, there are many factors that can be manipulated to improve the image SNR, but for fMRI, the most significant ones include lowering the spatial resolution (increasing V), using a high field strength magnet (B_0), lengthening imaging times (increasing $T_{A/D}$).

Depending on the spatial resolution and field strength, however, other sources of noise may be more important. In these cases, the traditional methods for improving the signal-to-noise ratio, such as using larger voxels, may offer only a small improvement to the fMRI data. These other sources of noise in functional MRI experiments are not as easily understood and new methods must be developed to correct for their effects. For example, one approach to minimizing the undesired effects of cardiac and respiratory variability and head movement is to use rapid acquisition techniques such as echo-planar imaging (EPI) [3, 4] and spiral imaging [13]. Rapid imaging allows physiological motion to be frozen so that it does contribute to intra-image data inconsistency. It also allows for a large number of images to be averaged in an attempt to reduce the undesired physiologic variations. Other approach to address pulmonary and cardiac noise are to gate or reorder data acquisition according the phases of the physiological cycle. It is also possible to acquire information about the physiological effects during at each acquisition and use this information to correct the data as part of the image reconstruction process [14-16].

The elimination of the effects of head movement represents another challenge for functional MRI experiments. Many experimenters use some form of head restraint, such as bite-bars (subject bites into a preformed dental mold) foam packing, or surgical pillows (a pillow that hardens and retains shape after evacuation of air). All of these methods work to some extent, though it is also important to properly instruct the patient not to move. Finally, head movement can be estimated and mostly corrected in post-processing by a number of methods [17-20].

Specific steps can be taken to reduce the effects of slow drifts in the MRI signal as well as head movement. One way to address these considerations is to repeat each behavioral state multiple times and ordering these states in an alternating, counter-balanced, or randomized ordering. These condition ordering schemes can also be used to address trends related subject performance and learning throughout the experiment . Post-processing strategies include removal of linear (high pass filtering) order drifts terms prior to statistical analyses and normalization of global image intensities.

Image Acquisition Issues

As discussed above, the ability to freeze motion is a strong motivating factor for using rapid imaging methods for fMRI acquisition. In addition, accurately tracking time-course of fMRI changes requires rapid sampling for each slice (e.g. at least once every 2 or 3 seconds). Combined with the common need to study the whole brain, rapid imaging methods have been and will continue to be the dominant way of acquiring fMRI data. The most common methods for fMRI are the single-shot, T2*-weighted methods like single-shot EPI and spiral imaging. While these methods are very fast and possess the good T2*-weighting, they are also prone to su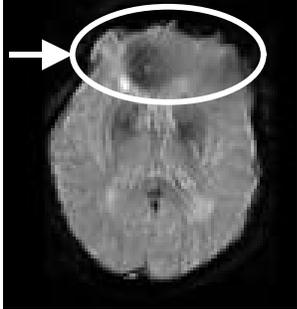sceptibility distortions and blurring as shown in Figure 10. In addition, the use of higher field strengths (3 and 4 Tesla) for fMRI only increases the size of these distortions. There are several approaches to addressing these distortions. First, a variety of post-processing techniques to correct for some of the distortion do exist and help to some extent [21-24]. In addition, higher performance gradient systems also reduce distortions by increasing the bandwidth of the acquisition (which reducing the susceptibility effects relative to the overall bandwidth). Finally, the use of multi-shot variants can reduce distortions at the expense of image acquisition time (temporal resolution). When using multi-shot techniques, however, one must also be aware of the potential for increased signal variations due to physiological fluctuations and head movement.

Figure 10. Demonstration of susceptibility distortions in EPI.

Signal Temporal Characteristics

In addition to the noise processes, it is important to consider the temporal dynamics of the activation response when design experiments and processing strategies. The MRI response is delayed and relatively slow compared to actual brain activity. There are a number of factors associated with temporal response of the deoxy-Hb effect, however, it is commonly reported to take 6-9 s to reach peak and 8-20 seconds to return to base line intensity. Negative responses following a block of activity are commonly seen and while not widely replicated, some groups have reported an initial negative response 500-2500 ms after activity begins. Figure 11 contains a drawing of a typical temporal response to neuronal activity. This temporal response must be considered when designing appropriate processing strategies, assigning images to particular behavioral states or transition regions, and detecting short duration states. This is also important for experimental design. For example, when alternating between two behavioral states, the temporal response results in a cutoff frequency of approximately 1 cycle / 12 s.
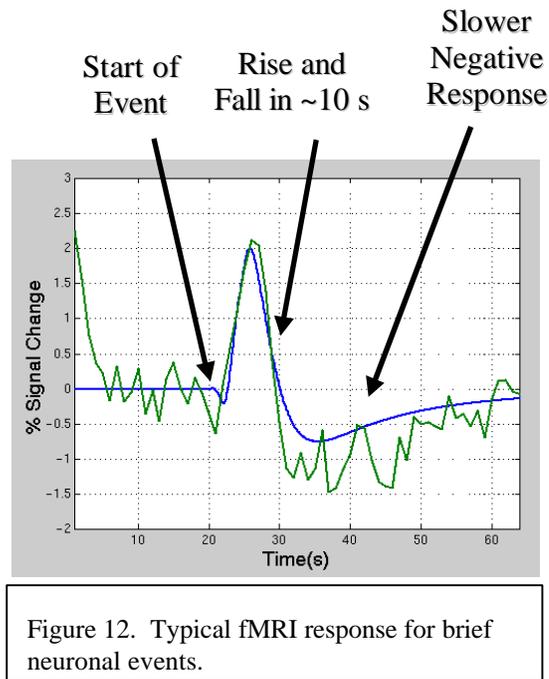
Figure 12. Typical fMRI response for brief neuronal events.
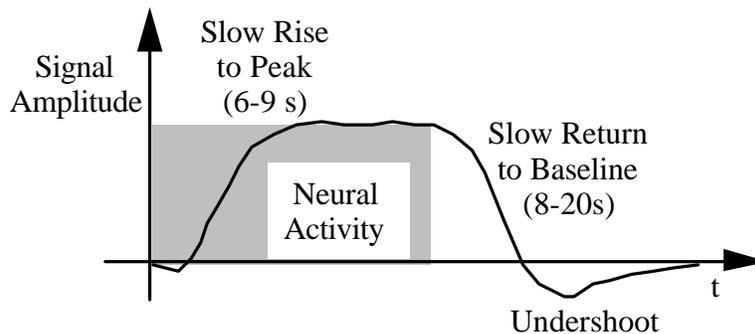
Figure 11. Typical time course for activation related signals in T_2*-weighted (BOLD) functional MRI.

Event-Related Functional MRI

A recent development in functional MRI is the imaging of the responses to individual trials, known as event-related fMRI or single-trial [25-28]. Above (Figure 11), we described the response to a block of trials all of the same kind (e.g. a continuous string of finger movements). Because the hemodynamic response is rather slow, the responses all blur together to exhibit roughly a constant response size in the central portion of the block. In event-related fMRI, the responses to individual trials are examined. This is done by using an experimental designs that allows these responses to be extracted. For example, the inter-trial interval (ITI) can be extended to allow the response to arrive and dissipate before the next trial is given (this is usually 10-12 seconds, but can be longer if task being executed in the trial is rather long). Individual responses can also be extracted by randomly mixing the trial types or randomizing the ITI, but allowing the responses to overlap. When this is done, fluctuations in the signal intensity result from the summation of responses of differing sizes to the mixed trial types or from the summation of the responses to randomly timed trials. The estimation of the response location, size and shape in event-related fMRI is presently an active area for research. A complicating factor in the analysis is that the assumed shape of the hemodynamic response can greatly affect the fMRI analysis, perhaps necessitating the acquisition of information regarding the hemodynamic response. This powerful new approach to fMRI allows considerably more flexibility in the design of fMRI paradigms and allows separation of effects based on stimulus type, response type, reaction time, etc. For example, subject errors can be analyzed separately than correct responses and the response to rare events can be separated from common events.

Statistical Testing

One critical step in any functional MRI study is the statistical testing, thresholding and result compilation. In general, once images have been through a variety of preprocessing stages (e.g. image reconstruction, distortion removal, movement correction, etc.), general statistical analysis can be applied (for a review see [29]). The most commonly applied methods are the linear parametric methods, which include such methods as t-test, cross-correlation, ANOVA, and the general linear

model (multiple regression) [30]. There methods are easy to use and can easily give measures of statistical significance, but have more restrictive assumptions about the fMRI response timing and shape and about the noise characteristics. Non-linear parametric methods, for example, are less restrictive and can be used to estimate the parameters regarding the shape of the response [31]. At the far other extreme are methods that do not even require assumptions about the times that the activation begins and ends [32-34].

After initial statistical testing, the data are queried according the kind of information to be derived. Often, a specific hypothesis is posed that a particular regions involved with the performance of a particular task. In these cases, one may identify the regions of interest and evaluate the statistical test over those regions. In other cases, there is no *a priori* expectation of the regions that are involved. In these cases, similar methods are used considering the whole brain as a region of interest, but that statistical analysis is must be more conservative (higher statistical threshold) since there is an increased chance the random pixels will considered to be active. Finally, the data need to be made available for use by the end user. This often means placing the data in a standard atlas (e.g. Taliarch coordinates [35]) or by overlaying the functional information onto an anatomical frame of reference. There are numerous packages, some free – some not, available from university and government sites, major equipment manufacturers, and private companies for processing fMRI data. Most of these packages have capabilities for movement correction, statistical analysis and display.

References

1. Ogawa, S., T. Lee, A. Nayak, and P. Glynn, Oxygenation-sensitive contrast in magnetic resonance image of rodent brain at high magnetic fields. *Magn Reson Med*, 1990. **14**: p. 68-78.
2. Ogawa, S., D.W. Tank, R. Menon, *et al.*, Intrinsic signal changes accompanying sensory stimulation: Functional brain mapping with magnetic resonance imaging. *Proc. Natl. Acad. Sci., USA*, 1992. **89**: p. 5951-5955.
3. Bandettini, P.A., E.C. Wong, R.S. Hinks, R.S. Tikofsky, and J.S. Hyde, Time course EPI of human brain function during task activation. *Magn. Reson. Med.*, 1992. **25**: p. 390-397.
4. Kwong, K.K., J.W. Belliveau, D.A. Chesler, *et al.*, Dynamic magnetic resonance imaging of human brain activity during primary sensory stimulation. *Proc. Natl. Acad. Sci., USA*, 1992. **89**: p. 5675-5679.
5. Lauterbur, P.C., Image formation by induced local interactions: examples employing nuclear magnetic resonance. *Nature*, 1973. **242**: p. 190-191.
6. Mansfield, P., Multi-planar image formation using NMR spin echoes. *J Phys C*, 1977. **10**: p. L55-L58.
7. Mansfield, P. and I.L. Pykett, Biological and medical imaging by NMR. *J. Magn. Reson.*, 1978. **29**: p. 355-373.
8. Likes, R.S. Moving gradient zeugmatography. U.S. Patent 4,307,343, 1981.
9. Ljunggren, S., A Simple Graphical Representation of Fourier-Based Imaging Methods. *J. Magn. Reson.*, 1983. **54**: p. 338-343.
10. Twieg, D., The k-trajectory formulation of the NMR imaging process with application in analysis and synthesis of imaging methods. *Med Phys*, 1983. **10**: p. 610-621.
11. Roy, C.S. and C.S. Sherrington, On the regulation of the blood-supply of the brain. *J Physiol (London)*, 1890. **11**: p. 85-108.
12. Springer, C.S., C.S. Patlak, I. Palyka, and W. Huang, Principles of susceptibility constrast-based functional MRI: The sign of the functional MRI response, in *Functional MRI*, C.W.T. Moonen and P.A. Bandettini, Editors. 1999, Springer-Verlag: Berlin. p. 91-102.
13. Noll, D.C., J.D. Cohen, C.H. Meyer, and W. Schneider, Spiral K-space MR Imaging of Cortical Activation. *J. Magn. Reson. Imaging*, 1995. **5**: p. 49-56.

14. Hu, X. and S.-G. Kim, Reduction of Signal Fluctuations in Functional MRI Using Navigator Echoes. *Magn. Reson. Med.*, 1994. **31**: p. 495-503.

15. Hu, X., T.H. Le, T. Parrish, and P. Erhard, Retrospective Estimation and Correction of Physiological Fluctuation in Functional MRI. *Magnetic Resonance in Medicine*, 1995. **34**: p. 201-212.

16. Noll, D.C. and W. Schneider. Theory, simulation, and compensation of physiological motion artifacts in functional MRI. in *IEEE Int. Conf. on Image Proc.* 1994. Austin, TX. p. 40-44.

17. Woods, R.P., S.T. Grafton, C.J. Holmes, S.R. Cherry, and J.C. Mazziotta, Automated image registration: I. General methods and intrasubject. *Journal of Computer Assisted Tomography*, 1998. **22**(1): p. 139-52.

18. Wood, M.L., M.J. Shiviji, and P.L. Stanchev, Planar-motion correction with use of k-space data acquired in Fourier MR imaging. *J. Magn. Reson. Imaging*, 1995. **5**: p. 57-64.

19. Eddy, W.F., M. Fitzgerald, and D.C. Noll, Improved image registration using Fourier domain interpolation. *Magn. Reson. Med.*, 1996. **36**: p. 923-931.

20. Ashburner, J. and K.J. Friston, Image Registration, in *Functional MRI*, C.W.T. Moonen and P.A. Bandettini, Editors. 1999, Springer-Verlag: Berlin. p. 286-299.

21. Weisskoff, R. and T. Davis. Correcting Gross Distortion on Echo Planar Images. in *11th Ann. Sci. Mtg. Soc. of Magn. Reson. in Med.* 1992. Berlin, Germany. p. 4515.

22. Jezzard, P. and R.S. Balaban, Correction for geometric distortion in echo planar imagnes from B0 variations. *Magn Reson Med*, 1995. **34**: p. 65-73.

23. Kadah, Y.M. and X. Hu, Simulated phase evolution rewinding (SPHERE): a technique for reducing B0 inhomogeneity effects in MR images. *Magnetic Resonance in Medicine*, 1997. **38**(4): p. 615-27.

24. Noll, D.C., C.H. Meyer, J.M. Pauly, D.G. Nishimura, and A. Macovski, A homogeneity correction method for magnetic resonance imaging with time-varying gradients. *IEEE Trans. Med. Imaging*, 1991. **10**(4): p. 629-637.

25. Buckner, R.L., P.A. Bandettini, K.M. O'Craven, *et al.*, Detection of cortical activation during averaged single trials of a cognitive task using functional magnetic resonance imaging. *Proc. Natl. Acad. Sci.*, 1996. **93**: p. 14878-14883.

26. Cohen, J.D., W.M. Perlstein, T.S. Braver, *et al.*, Temporal dynamics of brain activation during a working memory task. *Nature*, 1997. **386**: p. 604-608.

27. Courtney, S.M., L.G. Ungerleider, K. Keil, and J.V. Haxby, Hierarchical organization of a distributed extrastiate-prefontal system for human working memory. *Nature*, 1997. **386**: p. 608-611.

28. McCarthy, G., L. Luby, J. Gore, and P. Goldman-Rakic, Infrequent events transiently activate human prefrontal and parietal cortex as measured by functional MRI. *J Neurophysiology*, 1997. **77**: p. 1630-1634.

29. Lange, N., Statistical Procedures for Functional MRI, in *Functional MRI*, C.W.T. Moonen and P.A. Bandettini, Editors. 1999, Springer-Verlag: Berlin. p. 301-335.

30. Friston, K.J., A.P. Holmes, K.J. Worsley, *et al.*, Statistical Parametric Maps in Functional Imaging: A General Linear Approach. *Human Brain Mapping*, 1995. **2**: p. 189-210.

31. Genovese, C.R. Statistical inference in functional magnetic resonance imaging. Carnegie Mellon University, Statistics Tech Report 674, 1998.

32. Baumgartner, R., C. Windischberger, and E. Moser, Quantification in functional magnetic resonance imaging: fuzzy clustering vs. correlation analysis. *Magnetic Resonance Imaging*, 1998. **16**(2): p. 115-25.

33. Weaver, J.B., Efficient calculation of the principal components of imaging data. *Journal of Cerebral Blood Flow & Metabolism*, 1995. **15**(5): p. 892-4.

34. McKeown, M.J., S. Makeig, G.G. Brown, *et al.*, Analysis of fMRI data by blind separation into independent spatial components. *Human Brain Mapping*, 1998. **6**(3): p. 160-88.

35. Talairach, J. and P. Tournoux, Co-Planar Stereotaxic Atlas of the Numan Brain: 3D Proportional System: An Approach to Cerebral Imaging. 1988, New York: Georg Thieme Verlag.